Advanced Materials
Manufacturing & Characterization

journal home page: www.ijammc-griet.com

Nonlinear Fatigue Crack Growth Analysis of a Center Crack Plate by XFEM

I. V. Singh, B. K. Mishra, Sachin Kumar, A. S. Shedbale

Department of Mechanical and Industrial Engineering, Indian Institute of Technology Roorkee, Roorkee, U.K., INDIA

ARTICLE INFO

Keywords:
XFEM, LEFM, EPFM,
J-integral, SIF,
Von-Mises yield criterion,
Holes, inclusions and minor cracks

ABSTRACT

In the present article, the fatigue life of a center crack plate has been evaluated using XFEM in the presence of defects (holes, inclusions and minor cracks). The effect of plasticity is also evaluated on the fatigue life of the components. A generalized Ramberg-Osgood material model has been used to model the stress-strain behavior of the material. Von-Mises yield criterion has been used with isotropic strain hardening. A domain based approach is used to calculate the values of *J*-integral for two fracture modes (mode-I and mode-II). The values of stress intensity factor are evaluated from the *J*-integral values. Paris law is used to calculate the fatigue life under cyclic loading. Finally, the results obtained by linear and elasto-plastic analysis are compared with each other.

Introduction

All material used for engineering purposes are heterogeneous in nature in some way. The heterogeneous nature of the material arises due to the presence of defects i.e. pores, inclusions and cracks, etc. Therefore, the crack growth behavior has become a major issue to ensure the reliability and to avoid the catastrophic consequences of the structures/components. In such cases, the structures/components, subjected to cyclic loading may sometimes lead to the fatigue failure. Thus, there is need to accurately analyze such structures/components to get better service throughout their lifespan. During cyclic loading, the fatigue life of a component is highly influenced by the plasticity induced crack closure (PICC) phenomenon [1]. The primary source for the PICC is the plasticity ahead of the crack tip. During loading, a considerable amount of plastic strains is developed near the crack tip, which is not fully reversible upon unloading. Thus, some residual plastic strains remains near the crack tip at the minimum load. These residual plastic strains develop the plastic wake behind the crack tip as the crack extends. This phenomenon leads to the formation of compressive region near the crack tip, which tends to close the crack tip. Therefore, for the next loading cycle, some applied tensile load consumed to overcome the residual stresses at the crack tip, which reduces the crack driving force for the further fatigue crack growth.

Nowadays, numerous methods have been developed to model the fracture mechanics problems such as boundary element method (BEM) [2], finite element method (FEM) [3], meshfree methods [4], and extended finite element method (XFEM) [5-6]. Though, the FEM has been widely used for the simulation of crack growth problems but it has got some drawbacks e.g. it needs a conformal mesh to model the crack and requires remeshing at each stage of crack propagation, which is quite cumbersome. Also, to capture the stress singularity at the crack tip, it requires some special elements. Therefore, XFEM has been extensively used to model the crack growth problems in fracture mechanics. In this method, the requirement of conformal mesh is eliminated and the modeling of crack growth and other arbitrary discontinuities (voids, inclusions and minor cracks) are performed by adding some enrichment terms [5] to the standard finite element approximation.

It has been observed that the fatigue life of the components/ structures is affected due to the presence of flaws. The linear analysis of the fatigue life for a cracked plate is already carried out by Singh et al. [7] in the presence of multiple flaws. In the present work, the elasto-plastic fatigue life simulations have been performed for a center cracked plate in the presence of multiple defects (voids, inclusions and minor cracks). Under cyclic loading,

• Corresponding author: I.V. Singh
• E-mail address: ivsingh@gmail.com
• Doi: http://dx.doi.org/10.11127/ijammc.2014.03.02

the crack closure phenomenon is modeled by allowing the crack face nodes to move in negative direction, which develops the compressive stresses near the crack tip. The domain based approach is used for evaluating the *J*-integral for mode-I and mode-II. The small strain plasticity is assumed to model the plastic behavior of the material. Hence, the stress intensity factor values are obtained from *J*-integral values using linear elastic relations. Crack growth direction is determined using the maximum principal stress criterion [4, 7]. Two example problems are solved by XFEM using linear elastic and elasto-plastic material behavior. The results obtained for two different material behaviors are compared with each other.

Numerical Formulation

Governing equations

The governing equations in the presence of internal defects are briefly revised, and the equilibrium equation [4-5] can be written as,

$$\nabla.\boldsymbol{\sigma} + \mathbf{b} = \mathbf{0} \text{ in } \Omega \tag{1}$$

where $\boldsymbol{\sigma}$ is a Cauchy stress tensor and $\mathbf{b}$ is the body force per unit volume. In this work, the plastic potential function and yield function are identical. Thus, the expression for plastic strain increment and incremental stress-strain relations can be written as [8].

$$(d\varepsilon_{ij})^p = d\lambda \frac{\partial Q}{\partial \sigma_{ij}} \text{ and } d\boldsymbol{\sigma} = \mathbf{D}_{ep} d\boldsymbol{\varepsilon} \tag{2}$$

For associated theory of plasticity [9], the elasto-plastic constitutive matrix ($\mathbf{D}_{ep}$) becomes symmetric. However, for non-associated theory, the elasto-plastic constitutive matrix becomes un-symmetric.

Weak formulation

The weak form of governing equations can be written as [5, 7],

$$\int_{\Omega} \boldsymbol{\sigma}(\mathbf{u}) : \boldsymbol{\varepsilon}(\mathbf{v}) d\Omega = \int_{\Omega} \mathbf{b}.\mathbf{v} d\Omega + \int_{\Gamma_t} \bar{\mathbf{t}}.\mathbf{v} d\Gamma \tag{3}$$

After substituting the trial and test functions and using the arbitrariness of nodal variations, the following discrete system of equations are obtained,

$$\left[\mathbf{K}\right]\{\mathbf{d}\} = \{\mathbf{f}\} \tag{4}$$

where, $\mathbf{K}$ is the global stiffness matrix, $\mathbf{d}$ is the vector of nodal unknowns and $\mathbf{f}$ is the external force vector.

Displacement approximation for crack, inclusions and holes

At a particular node of interest $\mathbf{x}_i$, the displacement approximation for 2-D body having multiple discontinuities such as cracks, inclusions and holes can be written as [5-6-7],

$$\mathbf{u}^h(\mathbf{x}) = \sum_{i=1}^{n} N_i(\mathbf{x}) \left\{ \bar{\mathbf{u}}_i + \underbrace{\left[H(\mathbf{x}) - H(\mathbf{x}_i)\right]\mathbf{a}_i}_{i \in n_r} + \underbrace{\sum_{\alpha=1}^{4} \left[\beta_\alpha(\mathbf{x}) - \beta_\alpha(\mathbf{x}_i)\right]\mathbf{b}_i^\alpha}_{i \in n_A} \right\} + \sum_{i=1}^{n} N_i(\mathbf{x}) \left\{ \underbrace{\phi(\mathbf{x})\mathbf{c}_i}_{i \in n_i} + \underbrace{\left[\psi(\mathbf{x}) - \psi(\mathbf{x}_i)\right]\mathbf{d}_i}_{i \in n_h} \right\} \tag{5}$$

where $\bar{\mathbf{u}}_i$ is the nodal displacement vector associated with the continuous part of the FE solution; n is a set of all nodes in the mesh; n_r and n_A are set of nodes belonging to those elements which are completely and partially cut by the crack respectively; $H(\mathbf{x})$ is the Heaviside function, defined for those elements, which are completely cut by the crack and it takes the value +1 on one side and -1 on other side of the crack. $\beta_\alpha(\mathbf{x})$ are the asymptotic crack tip enrichment functions given in [7,10] for linear elastic and elasto-plastic analysis; $\mathbf{a}_i$ and $\mathbf{b}_i^\alpha$ are the enriched nodal DOF's associated with $H(\mathbf{x})$ and $\beta_\alpha(\mathbf{x})$ respectively; n_i and n_h are the set of nodes belonging to those elements which are cut by inclusions and holes respectively; $\phi(\mathbf{x})$ and $\psi(\mathbf{x})$ are the level set function and Heaviside function respectively and $\mathbf{c}_i$ and $\mathbf{d}_i$ are respective enriched DOF's associated with them.

The elemental matrices $\mathbf{k}$ and $\mathbf{f}$ in Eq. 4, are obtained using the approximation function defined in Eq. 5,

$$\mathbf{k}_{ij}^e = \begin{bmatrix} \mathbf{k}_{ij}^{uu} & \mathbf{k}_{ij}^{ua} & \mathbf{k}_{ij}^{ub} & \mathbf{k}_{ij}^{uc} & \mathbf{k}_{ij}^{ud} \\ \mathbf{k}_{ij}^{au} & \mathbf{k}_{ij}^{aa} & \mathbf{k}_{ij}^{ab} & \mathbf{k}_{ij}^{ac} & \mathbf{k}_{ij}^{ad} \\ \mathbf{k}_{ij}^{bu} & \mathbf{k}_{ij}^{ba} & \mathbf{k}_{ij}^{bb} & \mathbf{k}_{ij}^{bc} & \mathbf{k}_{ij}^{bd} \\ \mathbf{k}_{ij}^{cu} & \mathbf{k}_{ij}^{ca} & \mathbf{k}_{ij}^{cb} & \mathbf{k}_{ij}^{cc} & \mathbf{k}_{ij}^{cd} \\ \mathbf{k}_{ij}^{du} & \mathbf{k}_{ij}^{da} & \mathbf{k}_{ij}^{db} & \mathbf{k}_{ij}^{dc} & \mathbf{k}_{ij}^{dd} \end{bmatrix} \tag{6}$$

$$\mathbf{k}_{ij}^{rs} = \int_{\Omega^e} (\mathbf{B}_i^r)^T \mathbf{C} \mathbf{B}_j^s h d\Omega \text{ where } r,s = u,a,b,c,d \tag{7}$$

$$\mathbf{f}^h = \left\{ \mathbf{f}_i^u \ \mathbf{f}_i^a \ \mathbf{f}_i^{b1} \ \mathbf{f}_i^{b2} \ \mathbf{f}_i^{b3} \ \mathbf{f}_i^{b4} \ \mathbf{f}_i^c \ \mathbf{f}_i^d \right\}^T \tag{8}$$

The expressions of force vectors for a crack are given by Singh et al. [7], similarly the force vector associated with holes and inclusions can be written as,

$$\mathbf{f}_i^c = \int_{\Omega^e} N_i \phi(\mathbf{x}) \, \mathbf{b} d\Omega + \int_{\Gamma_t} N_i \phi(\mathbf{x}) \, \bar{\mathbf{t}} \, d\Gamma \tag{9}$$

$$\mathbf{f}_i^d = \int_{\Omega^e} N_i \left(\psi(\mathbf{x}) - \psi(\mathbf{x}_i)\right) \mathbf{b} d\Omega + \int_{\Gamma_t} N_i \left(\psi(\mathbf{x}) - \psi(\mathbf{x}_i)\right) \bar{\mathbf{t}} \, d\Gamma \tag{10}$$

where, N_i are finite element shape function, $\mathbf{B}_i^u$, $\mathbf{B}_i^a$, $\mathbf{B}_i^b$, $\mathbf{B}_i^{b\alpha}$, $\mathbf{B}_i^c$ and $\mathbf{B}_i^d$ are the matrices of shape function derivatives. The expressions of $\mathbf{B}_i^u$, $\mathbf{B}_i^a$, $\mathbf{B}_i^b$ and $\mathbf{B}_i^{b\alpha}$ matrices are given by Singh et al. [7], thus, in similar way the matrices of shape function derivatives associated with the holes and inclusions can be written as,

$$\mathrm{B}_i^c = \begin{bmatrix} \left(N_i\,\phi(\mathbf{x})\right)_{,x} & 0 \\ 0 & \left(N_i\,\phi(\mathbf{x})\right)_{,y} \\ \left(N_i\,\phi(\mathbf{x})\right)_{,y} & \left(N_i\,\phi(\mathbf{x})\right)_{,x} \end{bmatrix} \tag{11}$$

$$\mathrm{B}_i^d = \begin{bmatrix} \left(N_i\left(\psi(\mathbf{x})-\psi(\mathbf{x}_i)\right)\right)_{,x} & 0 \\ 0 & \left(N_i\left(\psi(\mathbf{x})-\psi(\mathbf{x}_i)\right)\right)_{,y} \\ \left(N_i\left(\psi(\mathbf{x})-\psi(\mathbf{x}_i)\right)\right)_{,y} & \left(N_i\left(\psi(\mathbf{x})-\psi(\mathbf{x}_i)\right)\right)_{,x} \end{bmatrix} \tag{12}$$

Computation of Stress Intensity Factor and Fatigue Life

In this paper, the plastic behavior of the material is modeled using Ramberg-Osgood equation [11].

$$\varepsilon = \frac{\sigma}{E} + \left(\frac{\sigma}{\bar{H}}\right)^{1/\bar{n}} \tag{13}$$

where, $\bar{H}$ is the strength coefficient and $\bar{n}$ is the strain hardening exponent. In the presence of plasticity, Hutchinson-Rice-Rosengren (HRR) singularity [12-13] is developed at the crack tip. Therefore, the stress intensity factor values cannot be obtained directly for the elasto-plastic analysis. Thus, the *J*-integral values are obtained for different modes by domain based approach. The modes are separated by decomposing the near crack tip fields into their symmetric and anti-symmetric parts [15-16] with respect to crack tip. In this work, small strain plasticity is assumed, hence, the stress intensity factors for mode-I and mode-II can be obtained from *J*-integral values using linear elastic relations.

The *J*-integral in an equivalent area integral form can be written as [14],

$$J = \int_A \left[\sigma_{ij}\frac{\partial u_i}{\partial x_1} - W\delta_{ij}\right]\frac{\partial q_1}{\partial x_j}\,dA \tag{14}$$

where, $W = \int_0^{\varepsilon_{ij}} \sigma_{ij}\,d\varepsilon_{ij}$ is the strain energy density; σ_{ij} is the stress tensor; u_i is displacement field vector; δ_{ij} is the Kronecker's delta; A is an area that contains both the top and bottom crack faces; q is a function that is unity along the inner boundary of A and zero along the outer boundary.

The maximum principal stress criterion has been employed to obtain the direction of the crack growth. Therefore, the local direction of crack growth (θ_c) is obtained by [7, 17],

$$\theta_c = 2\tan^{-1}\left(\frac{K_I - \sqrt{K_I^2 + 8K_{II}^2}}{4K_{II}}\right) \tag{15}$$

As per this criterion, the equivalent mode-I SIF can be obtained by,

$$K_{Ieq} = K_I\cos^3\left(\frac{\theta_c}{2}\right) - 3K_{II}\cos^2\left(\frac{\theta_c}{2}\right)\sin\left(\frac{\theta_c}{2}\right) \tag{16}$$

The fatigue life is obtained using the generalized Paris law [7, 18], which is defined as,

$$\frac{da}{dN} = C\left(\Delta K_{eff}\right)^m \tag{17}$$

where, the effective SIF in case of linear analysis and elasto-plastic analysis can be obtained as,

$$\Delta K_{eff} = \left(K_{Ieq}\right)_{\max} - \left(K_{Ieq}\right)_{\min} \tag{18}$$

$$\Delta K_{eff} = \left(K_{Ieq}\right)_{\max} - K_{\mathrm{res}} \tag{19}$$

where, K_{res} is the residual SIF due to the residual stresses near the crack tip at the minimum load, a is the crack length, N is the number of loading cycles, C and m are the Paris constant and Paris exponent respectively.

Numerical Results and Discussion

In this work, the elasto-plastic simulations of a center crack plate are performed by considering the generalized Ramberg-Osgood material model as given in Eq. 13. The material properties used for the simulations are given below [19].

Young's modulus of homogenous plate (E)	71.7 GPa
Poisson's ratio of homogenous plate (ν)	0.33
Young's modulus of inclusion (E_I)	20 GPa
Poisson's ratio of inclusion (ν_I)	0.30
Fracture toughness (K_{IC})	29 MPa$\sqrt{\mathrm{m}}$
Paris exponent (m)	3.21
Paris constant (C)	6.85 x 10^{-8}
Strain hardening exponent ($\bar{n}$)	0.0946

A homogenous rectangular plate of size 100 mm x 200 mm along with a center crack of length a = 20 mm is taken for the simulations. The plate is subjected to a cyclic tensile load of $\sigma_{\max}$ = 80 MPa and $\sigma_{\min}$ = 0 MPa at the top edge while the bottom edge is kept constrained in *y*-direction. A uniform mesh of size 60 nodes x 120 nodes is used to discretize the domain in *x* and *y*-directions respectively. The domain is discretized using four node Lagrangian quadrilateral elements. The higher order Gauss quadrature is used in the region near the discontinuity. A plane stress condition is assumed for the simulations.

Finite size rectangular plate with a center crack

In this case, a center crack of length, a = 20 mm is taken in the rectangular plate (100 mm x 200 mm) as shown in Figure 1. All the modeling conditions; loading, mesh size etc, are kept similar as explained above. In elasto-plastic analysis, compressive stresses develop near the crack tip during unloading, which leads to crack closure effect at the crack tip. Therefore, for the next loading step, some amount of the tensile load will be consumed to conquer these residual compressive stresses near the crack tip. This phenomenon reduces the crack driving forces. The variation

of SIF with crack length is shown in Figure 2. In this figure, three plots are given; one for the linear analysis using LEFM, second for the EPFM maximum and third for the EPFM residual. The values of SIFs for elasto-plastic analysis are higher as compared to the SIFs for linear elastic analysis due to the increase in effective crack length.

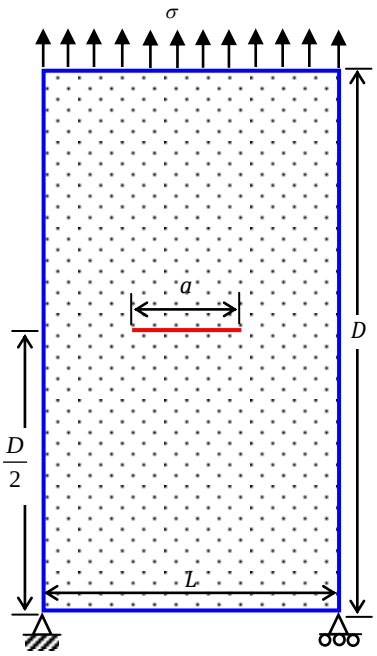

Figure 1. Center crack plate along with dimensions.

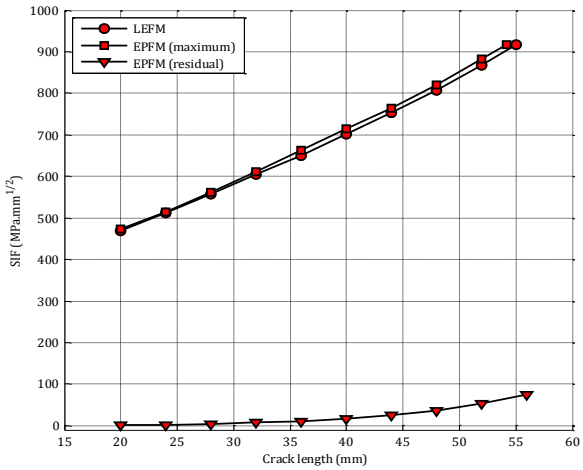

Figure 2. SIF variation with crack length for a center crack plate.

Further, to obtain the fatigue life for elasto-plastic analysis, the effective stress intensity factor values are obtained by subtracting the residual SIFs from the maximum SIFs. The variation of fatigue life with crack length is shown in Figure 3. The fatigue life is found to be 40511 cycles and 42430 cycles for linear elastic and elasto-plastic analysis respectively. Therefore, in case of elasto-plastic analysis, the fatigue life is increased by 4.5%. This increase may be attributed to the presence of residual compressive stresses during unloading.

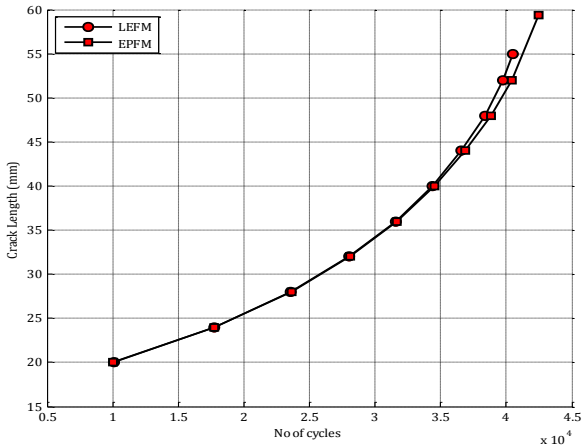

Figure 3. Fatigue life variation with crack length for a center crack plate.

Finite size rectangular plate with a center crack, holes, inclusions and minor cracks

In this case, a plate of size 100 mm x 200 mm along with a center crack of initial length a = 20 mm is taken for the simulation. To consider the effect of multiple defects on the fatigue life, holes, inclusions and minor cracks are randomly distributed in the plate as shown in Figure 4. The size of holes and inclusions are taken as arbitrary and their radii vary from 2.0 mm to 4.0 mm. The length of the minor cracks varies from 2.0 mm to 4.0 mm and orientation varies from -60° to 60°. The volume fraction of the defects is kept constant at 5%.

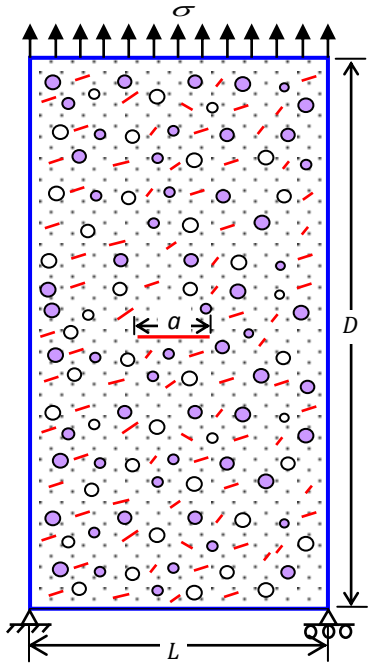

Figure 4. Center crack plate along with multiple holes, inclusions and minor cracks.

The variation of stress intensity factor and fatigue life against crack length is plotted in Figure 5 and Figure 6 respectively. In linear analysis, the fatigue life is found to be 31560 cycles

whereas, in case of elasto-plastic analysis, the fatigue life is found to be 33388 cycles. From the results, it is found that the fatigue life is increased by 5.5% for elasto-plastic analysis as compared to linear elastic analysis, whereas, multiple defects reduces the fatigue life by 22.1% and 21.3% for linear elastic and elasto-plastic analysis respectively. In elasto-plastic analysis, the increase in fatigue life is mainly due to the presence of residual compressive stresses during unloading.

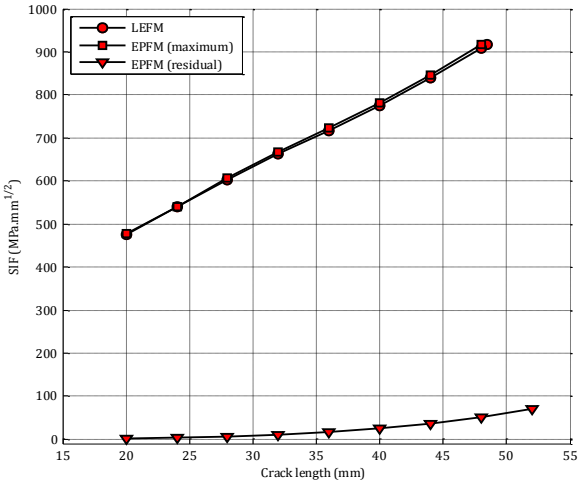

Figure 5. SIF variation with crack length for a center crack plate in the presence of multiple holes, inclusions and minor cracks.

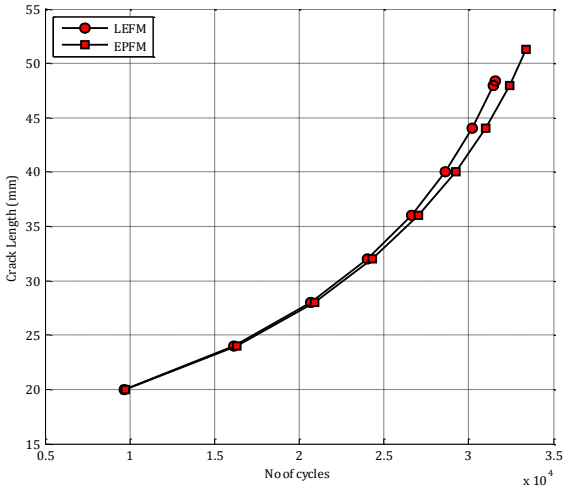

Figure 6. Fatigue life variation with crack length for a center crack plate in the presence of multiple holes, inclusions and minor cracks.

Conclusion

In this paper, the fatigue life of the plate is evaluated by XFEM in the presence of multiple defects using linear elastic and elasto-plastic material behavior. The stress-strain behavior of the material is modeled by Ramberg-Osgood equation. A Von-Mises yield criterion is used as a failure criterion along with isotropic strain hardening. The values of SIFs are obtained from the *J*-integral values for different modes using linear elastic relations. From the simulations, the following conclusions have been drawn:

- In elasto-plastic analysis, the plastic strains developed near the crack tip during loading are not fully reversible during unloading, which leads to the formation of residual compressive stresses at the crack tip.
- The residual compressive stresses develop a residual SIF, which reduces the crack driving force for the next loading cycle. Hence, plastic region at the crack tip improves the fatigue life.
- The presence of defects significantly affects the fatigue life.
- These simulations show that the XFEM can be easily extended to simulate 3-D elasto-plastic crack growth simulations in the presence of various defects.

References

1. Elber, W., Fatigue crack closure under cyclic tension, Engineering Fracture Mechanics, vol.2, pp.37–45, 1970.
2. Yan X., A boundary element modeling of fatigue crack growth in a plane elastic plate, Mechanics Research Communications, vol.33, pp.470–481, 2006.
3. Moes, N.,Dolbow, J., Belytschko, T., A finite element method for crack growth without remeshing, International Journal for Numerical Methods in Engineering, vol.46, pp.131–150, 1999.
4. Duflot, M., Dang, H. N., Fatigue crack growth analysis by an enriched meshless method, Journal of Computational and Applied Mathematics, vol.168,pp. 155–164,2004.
5. Belytschko, T., Black, T., Elastic crack growth in finite elements with minimal remeshing, International Journal for Numerical Methods in Engineering, vol.45, pp. 601–620, 1999.
6. Sukumar, N., Chopp, D.L., Moes, N., Belytschko, T., Modeling of holes and inclusions by level sets in the extended finite element method, Computer Methods in Applied Mechanics and Engineering, vol.190, pp.6183–6200,2001.
7. Singh, I.V., Mishra, B. K., Bhattacharya, S., Patil, R. U., The numerical simulation of fatigue crack growth using extended finite element method, International Journal of Fatigue, vol.36, pp.109–119,2012.
8. Hinton, E., Owen, D.R.J., Finite Element in Plasticity, Pineridge Press Ltd, Swansea, U. K., 1980.
9. Bland, D.R., The associated flow rule of plasticity, Journal of Mechanics and Physics of Solids, vol.6,pp.71–78, 1957.
10. Elguedj, T., Gravouil, A., Combescure, A., Appropriate extended functions for XFEM simulation of plastic fracture mechanics, Computer Methods in Applied Mechanics and Engineering, vol.195, pp. 501–515,2006.
11. Long, K.S., Experimental study of inelastic stress concentration around a circular notch, Naval Postgraduate School Monterey, California, 1996.
12. Hutchinson, J.W., Singular behavior at the end of a tensile crack in a hardening material, Journal of the Mechanics and Physics of Solids, vol.16, pp. 13–31,1968.
13. Rice, J.R., Rosengren, G F., Plane strain deformation near a crack tip in a power-law hardening material, Journal of the Mechanics and Physics of Solids, vol.16, pp.1–2, 1968.

14. Li, F.Z., Shih,C., Needleman, A., A comparison of methods for calculating energy release rates, Engineering Fracture Mechanics, vol.21, pp.405–421, 1985.
15. Ishikawa, H., A finite element analysis of stress intensity factors for combined tensile and shear loading by only a virtual crack extension, International Journal of fracture, vol.16, pp.243–246, 1980.
16. Bui, H.D., Associated path independent J-integrals for separating mixed modes, Journal of the Mechanics and Physics of Solids, vol.6, pp.439–448,1983.
17. Erdogan, F., Sih, G., On the crack extension in plates under plane loading and transverse shear, Journal of Basic Engineering, vol.85, 519–527, 1963.
18. Paris, P.C., Gomez, M.P., Anderson, W.E., A rational analytic theory of fatigue, The Trend in Engineering, vol.13,pp. 9–14,1961.
19. Aluminum 7075 T-6-ASM Material data sheet, asm.matweb.com